

Adaptive Modulation for Underwater Acoustic OFDM Communication

Suchi Barua, Yue Rong, Sven Nordholm, Peng Chen
 School of Electrical Engineering, Computing and Mathematical Sciences
 Curtin University, Bentley, WA 6102, Australia

Abstract— Rapidly varying multipath propagation and limitation of bandwidth are major constraints of underwater acoustic (UA) communication systems. In order to improve the spectral efficiency, adaptive modulation schemes are considered in the context of UA orthogonal frequency division multiplexing (OFDM) systems. The objective of this paper is developing self-adapting modulation algorithms by analyzing the characteristics of the UA channel and varying transmission parameters according to the channel condition. The signal-to-noise ratio (SNR) is estimated at the receiver and used as a performance metric to switch the modulation mode and fed back to the transmitter for data transmission. Simulation results show that the system performance is better than fixed modulation schemes.

Keywords— Adaptive modulation, time-varying channel, underwater acoustic communication.

I. INTRODUCTION

In the underwater acoustic (UA) communication channel, high speed communication remains a very challenging task because of limited bandwidth, fast time variations of the channel, extended multi-path, refractive properties of medium, severe fading and large Doppler shifts. Significant progresses have been made in UA communications in recent years with both single-carrier modulation and multicarrier modulation systems.

In this paper, multicarrier modulation is used in the form of orthogonal frequency division multiplexing (OFDM) and adaptive modulation and coding technique is considered in order to achieve high spectral efficiency in non-stationary UA environment. The use of adaptive modulation allows a system to choose a proper modulation depending on the channel conditions [1].

In non-adaptive (fixed) modulation, the transmitter does not exploit any information about the available channel parameters in choosing the modulation scheme. Alternatively, the channel information is made available to the transmitter in adaptive modulation and the performance of an adaptive modulation scheme depends on the transmitter's knowledge of the channel which is fed back from the receiver to the transmitter. In this paper, signal-to-noise ratio (SNR) is estimated at the receiver and used as channel state information (CSI) to choose the adaptive allocation of the transmission parameters. The transmitter then sends this information back to the transmitter for the next data frame. Different modulation constellations are selected based on the SNR for the next data frame and thus higher data rate and better spectral efficiency can be achieved.

In this paper, the effect of Doppler frequency in adaptive modulation is also studied. Adaptive modulation becomes

challenging with the increase of Doppler frequency which leads to significant inter-carrier interference (ICI). ICI deteriorates the system performance as it enhances the power of received signal in the inactive (null) subcarriers and also misleads the detection of transmitted signal on active subcarriers. Thus the ICI affects the estimation of SNR, which in turn affects the performance of adaptive modulation. In this paper, null subcarriers are used to facilitate estimation of carrier frequency offset (CFO).

We show in this paper that, the proposed adaptive modulation scheme increases the data rate of the UA communication systems and performs better for lower Doppler frequency i.e. for slowly moving transmitter and/or receiver. For rapidly moving transmitter and/or receiver, the ICI becomes more prominent. In the presence of ICI, the estimated noise power is not only due to the actual noise but also due to ICI which affects the SNR estimation. As the adaptive allocation of modulation constellations depends on the SNR estimation, the performance of the proposed adaptive modulation scheme deteriorates for higher Doppler frequency which means the adaptive UA communication system becomes limited by interference rather than by noise.

The rest of the paper is organised as follows. The system model is introduced in Section II. The channel model is presented in Section III. The adaptive modulation implementation is presented in Section IV. The simulation results are discussed in Section V. Conclusion is presented in Section VI.

II. SYSTEM MODEL

In this paper, we consider a frame-based coded UA OFDM communication system. The frame structure of the transmitted signals is shown in Fig. 1. Each block contains pilot subcarriers, null subcarriers and data subcarriers. We assume that pilot subcarriers are uniformly spaced [2, 3].

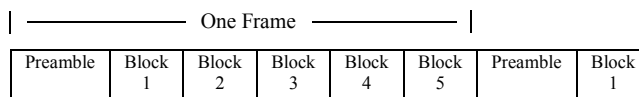


Fig. 1. Frame structure of the UA OFDM system.

In each frame, a binary source data stream $\mathbf{d} = (d[1], \dots, d[K_d])^T$ is generated, where $(\cdot)^T$ denotes the matrix (vector) transpose, K_d is the number of information-carrying bits in each frame. Each OFDM symbol is converted to the time domain by the inverse discrete Fourier transform (DFT), leading to the following baseband discrete time signal

$$\mathbf{x} = \mathbf{F}^H \mathbf{s} \quad (1)$$

where $(\cdot)^H$ denotes the conjugate transpose and \mathbf{F} is a $K_s \times K_s$ DFT matrix. $\mathbf{s} = (s[1], \dots, s[K_s])^T$ is the OFDM symbol vector mapped from \mathbf{d} depending on modulation constellations and K_s is the number of total subcarriers. The bandwidth of the transmitted signal is $B = f_{sc}K_s$, where f_{sc} is the subcarrier spacing. The duration of one OFDM symbol is $T = 1/f_{sc}$ and the total length of one OFDM block is $T_{total} = T + T_{cp}$, where T_{cp} is the length of cyclic prefix (CP). After removing the CP at the receiver end, the baseband discrete time samples of one OFDM symbol is

$$\mathbf{r}_t = \mathbf{P}\mathbf{F}^H\mathbf{S}\mathbf{F}\mathbf{h}_t + \mathbf{w}_t \quad (2)$$

where $\mathbf{S} = \text{diag}(\mathbf{s})$ is a diagonal matrix and $\mathbf{w}_t = (w[1], \dots, w[K_s])^T$ is the additive noise vector, \mathbf{h}_t is the discrete time domain representation of the channel impulse response (CIR) and $\mathbf{P} = \text{diag}(1, e^{-j2\pi\epsilon/B}, \dots, e^{-j2\pi(K_s-1)\epsilon/B})^T$ is the phase distortion caused by the Doppler shift and ϵ is CFO.

After estimating and removing the frequency offset, the frequency domain representation of the received signal is

$$\mathbf{r}_f = \mathbf{S}\mathbf{h}_f + \mathbf{w}_f \quad (3)$$

where \mathbf{w}_f is the additive noise vector in the frequency domain. $\mathbf{h}_f = (h_f[1], \dots, h_f[K_s])^T$ is a vector containing the channel frequency response (CFR) at all K_s subcarriers [3].

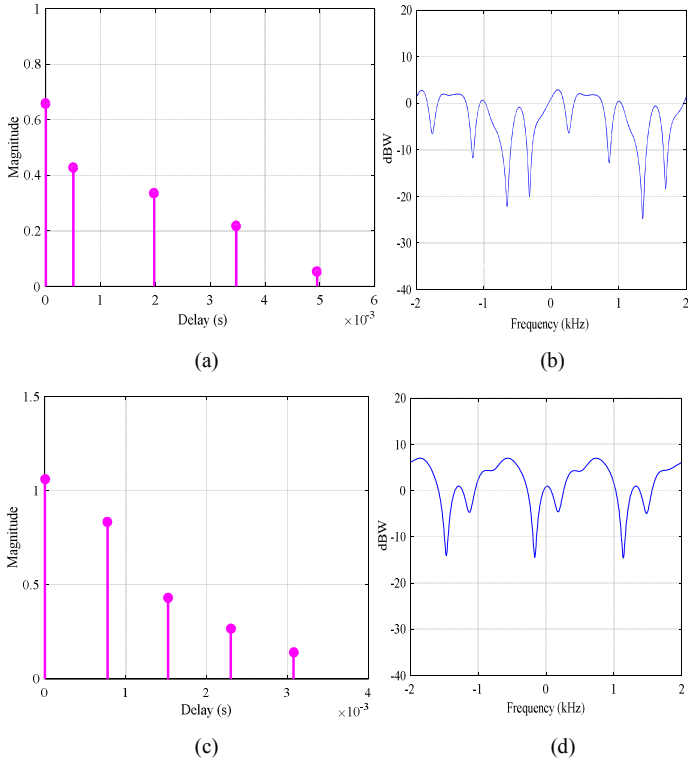


Fig. 2. CIRs and CFRs of the UA channel for 1st OFDM frame (a and b) and for 5th OFDM frame (c and d).

III. CHANNEL MODEL

UA communication is challenging because of the unique channel characteristics of UA channel and considered as one of

the most difficult communication channels due to the rapid dispersion in both time and frequency domain. UA channels are generally characterized by randomly time-varying multipath propagation which results in frequency selective fading [4]. Additionally, motion of the transmitter and/or receiver introduces Doppler shift to the channel which contributes to the changes in CIR. The CIR can be defined as

$$h(\tau, t) = \sum_{p=1}^{N_p} h_p(t)\delta(\tau - \tau_p(t)) \quad (4)$$

where N_p is the number of propagation path, τ is delay, $\delta(\cdot)$ is the Dirac delta function and t is the time at which the channel is observed. The coefficient $h_p(t)$ represents the gain of the p th path and $\tau_p(t)$ is the corresponding time-varying delay [5, 6].

Fig 2 depicts the time-varying CIRs and CFRs of the 1st and 5th OFDM frames. The channel gain is Rayleigh distributed at each path. Fig 2(a) and 2(c) show the time-varying behaviour of multipath channel where both the magnitude and the arrival time of the paths are varying. It is observed from 2(a) and 2(c) that, the magnitude of CIRs are varying fast between the first and the fifth frame. Fig 2(b) and 2(d) show the frequency selective fading as the power level varies over the signal bandwidth.

A. CFO Estimation

In this paper, adaptive modulation is investigated for different Doppler shifts by varying the relative velocity between the transmitter and the receiver. It is assumed that the motion of the transmitter and/or the receiver is causing the dominant Doppler shift. After removing CP from the received signal, CFO is estimated in null subcarriers in the receiver side. The CFO is performed in each OFDM block. The energy of the null subcarriers is used as the cost function.

$$J(\epsilon) = \|\Theta\mathbf{F}^H(\epsilon)\mathbf{r}_t\|^2 \quad (5)$$

where Θ is a selection matrix that picks the frequency-domain measurements on the null subcarriers out of all K_s subcarriers, $\|\cdot\|$ is the Euclidean norm of a vector, $\mathbf{F}(\epsilon) = \text{diag}(1, e^{j2\pi T_c\epsilon}, \dots, e^{j2\pi T_c(K_s-1)\epsilon})$ is diagonal matrix where T_c is the time interval for each sample. An estimation of ϵ is found through

$$\hat{\epsilon} = \text{argmin} J(\epsilon) \quad (6)$$

which is solved via 1-D search for ϵ [7].

The CFO estimation algorithm at null subcarriers performs better when the Doppler frequency is smaller. With the increase of Doppler frequency, the system performance decreases as the ICI at each subcarrier spills over from immediate adjacent subcarriers.

IV. ADAPTIVE MODULATION

Following the OFDM signal design, noise and received signal power is estimated in the frequency domain at the receiver. Received power at null subcarriers is used for noise variance estimation.

$$\hat{\sigma}_n^2 = \frac{1}{\bar{\mathcal{K}}_n} \sum_{m=1}^{\bar{\mathcal{K}}_n} |r_f[\mathcal{K}_n(m)]|^2 \quad (7)$$

where \mathcal{K}_n is the set containing the indices of null subcarriers and for a set \mathcal{X} , $\bar{\mathcal{X}}$ denotes the number of elements in \mathcal{X} and $r_f[m]$ is the frequency-domain received signal at the m th subcarrier. The SNR in the frequency domain can be estimated as

$$\bar{\gamma} = \frac{\frac{1}{\bar{\mathcal{K}}_a} \sum_{m=1}^{\bar{\mathcal{K}}_a} |r_f[\mathcal{K}_a(m)]|^2}{\frac{1}{\bar{\mathcal{K}}_n} \sum_{m=1}^{\bar{\mathcal{K}}_n} |r_f[\mathcal{K}_n(m)]|^2} - 1 \quad (8)$$

where \mathcal{K}_a is the set containing the indices of pilot and data subcarriers i.e. $\mathcal{K}_a = \mathcal{K}_p \cup \mathcal{K}_d$ [8]. The estimated SNR is used to choose the modulation mode adaptively. The chosen modulation mode is fed back to the transmitter for the next data frame.

The block diagram of the proposed adaptive modulation scheme in Fig. 3 shows that channel estimation and SNR estimation are done in the receiver side. Then a proper modulation mode is selected by the mode selector block depending on the estimated SNR for the next data frame. The selected modulation mode for the next data frame is fed back to the transmitter. The adaptive modulator block at the transmitter side consists of different modulators which provide different modulation mode and modulate the data frame according to the selected mode. The demodulator block demodulates the received signal according to the selected modulation mode.

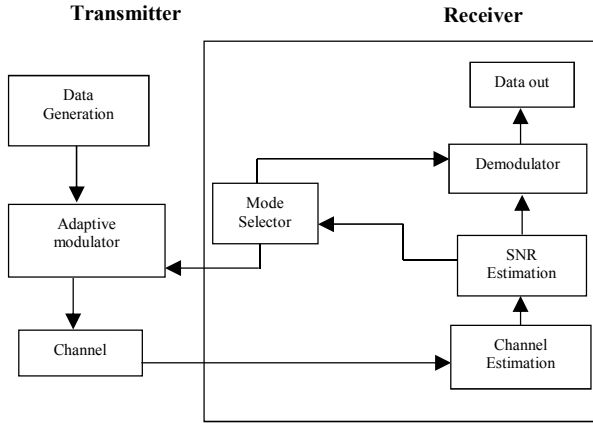


Fig. 3. Block diagram of adaptive modulation scheme.

In this work, the adaptation is done frame by frame. Individual modulation scheme results have been observed and analyzed for UA communication systems for fixed modulation. Extensive simulations of fixed modulation for different modulation schemes are used to select the target bit-error-rate (BER) and the estimated SNR is used as switching parameter [1, 9]. Switching threshold for adaptive modulation system is determined to keep the overall BER lower than the target BER. In fact, the highest modulation order is chosen under a certain BER and SNR. Therefore, a better tradeoff between data rate

and overall BER is achieved by the proposed adaptation system. Switching thresholds used for the adaptive modulation schemes are presented in Table I, Table II and Table III for Doppler frequency 0.0139 Hz, 0.1386 Hz and 1.3856 Hz respectively.

TABLE I. SWITCHING THRESHOLD FOR ADAPTIVE MODULATION SCHEMES FOR DOPPLER FREQUENCY 0.0139 HZ

Mode	Modulation	Threshold
1	BPSK	SNR < 15.6 dB
2	QPSK	15.6 dB ≤ SNR ≤ 21 dB
3	16QAM	SNR > 21 dB

TABLE II. SWITCHING THRESHOLD FOR ADAPTIVE MODULATION SCHEMES FOR DOPPLER FREQUENCY 0.1386 HZ

Mode	Modulation	Threshold
1	BPSK	SNR < 15.3 dB
2	QPSK	15.3 dB ≤ SNR ≤ 21.4 dB
3	16QAM	SNR > 21.4 dB

TABLE III. SWITCHING THRESHOLD FOR ADAPTIVE MODULATION SCHEMES FOR DOPPLER FREQUENCY 1.3856 HZ

Mode	Modulation	Threshold
1	BPSK	SNR < 7.7 dB
2	QPSK	7.7 dB ≤ SNR ≤ 15.5 dB
3	16QAM	SNR > 15.5 dB

TABLE IV. PARAMETERS USED IN SIMULATION

Bandwidth	$B = 4$ kHz
Number of subcarriers	$K_s = 512$
Subcarrier spacing	$f_{sc} = 7.8$ Hz
Length of OFDM symbol	$T = 128$ ms
Length of CP	$T_{cp} = 25$ ms
Number of pilot subcarriers	$K_p = 116$
Number of data subcarriers	$K_d = 332$
Number of null subcarriers	$K_n = 64$

V. SIMULATION RESULTS AND DISCUSSIONS

In the simulation, the performance of adaptive modulation is investigated in terms of the BER performance and data rate. The uncoded performance of fixed modulation has been studied based on BPSK, QPSK and 16QAM schemes. In the simulation, the UA OFDM system has 512 subcarriers in each block and the UA channel has 5 paths. Maximum Doppler shift varies from

0.0139 Hz to 1.3856 Hz. The system parameters used in the simulation are listed in Table IV.

In this work, adaptive modulation is performed depending on the SNR estimation. So, the SNR needs to be estimated as close as possible to the actual SNR. The SNR estimation algorithm performs better at lower Doppler frequency than the higher Doppler frequency because at higher Doppler frequency the estimated noise power increases due to ICI. Fig.4 shows the estimated SNR for different Doppler frequencies. It shows that, the SNR is estimated close to the actual SNR for lower Doppler frequency 0.0139 Hz and 0.1386 Hz which is seen from the diagonal upward straight line. However, the SNR is estimated close to the actual SNR up to 15dB for higher Doppler frequency 1.3856 Hz. The diagonal straight line starts to bend downward when SNR reaches above 15dB. Therefore, it can be said that, adaptive modulation can be performed at lower SNR (<15dB) for higher Doppler frequency.

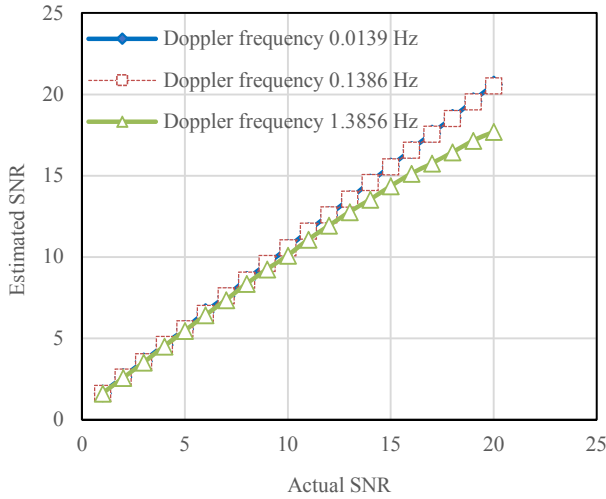


Fig. 4. Estimated SNR for different Doppler frequencies.

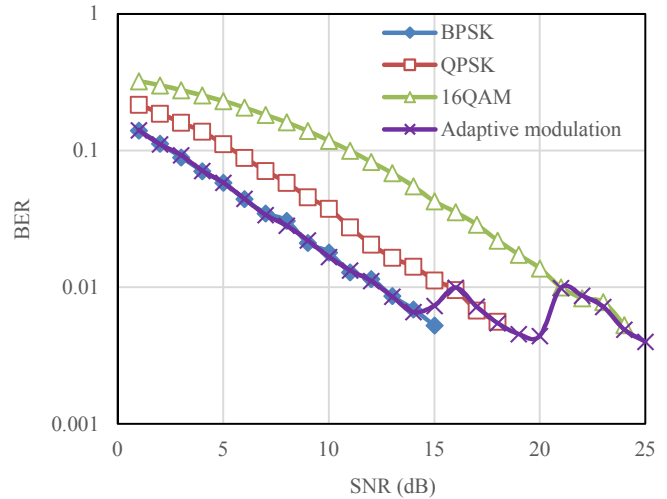
BER performance of adaptive modulation is compared to the BER performance of fixed modulation system as shown in Fig.5. When the Doppler frequency is low (0.0139 Hz and 0.1386 Hz), the system performs better and the target BER is chosen at 0.01 to perform adaptive modulation. For higher Doppler frequency (1.3856 Hz), the system performance deteriorates due to ICI which puts a limit on the SNR estimation for higher SNR; hence the target BER is chosen at 0.1 to perform adaptive modulation.

It also can be seen that, BER of adaptive modulation is better than the BER of fixed QPSK and QAM modulation schemes. The data rate of fixed modulation is fixed for each transmission. In this simulation the data rates of BPSK, QPSK and 16QAM are 1.86 kbps, 3.72 kbps and 7.44 kbps respectively. Alternatively, data rate of adaptive modulation changes in each transmission depending on the estimated SNR. The data rate of adaptive modulation is calculated 1.82 kbps and 1.79 kbps for Doppler shift of 0.0139 Hz and 0.1386 Hz respectively using 12500 frames for the SNR range of 1 to 25dB. The data rate of

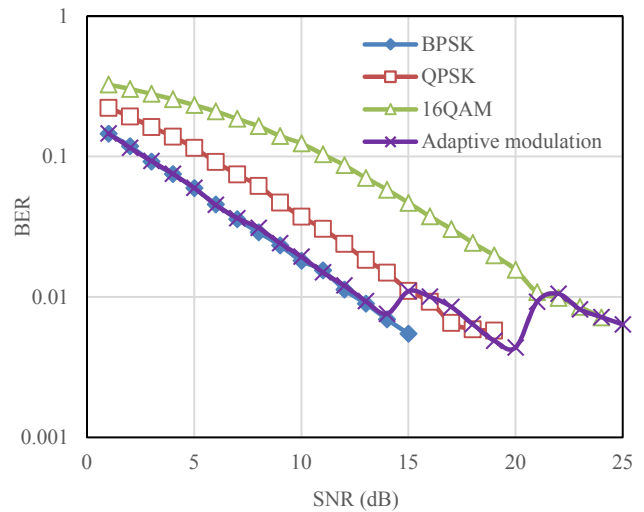
adaptive modulation for higher Doppler frequency 1.3856 Hz is calculated 2.02 kbps using 10000 frames for the SNR range of 1 to 20dB. It can be said that no fixed OFDM system can provide better BER performance while simultaneously providing better data rate. The proposed adaptive system can ensure higher data rate at target BER compared to fixed modulation.

VI. CONCLUSION

An adaptive modulation scheme is proposed in this paper which relies on the estimated SNR of the previous frame to choose adaptive allocation of the modulation mode for the next frame transmission. Extensive fixed modulation is investigated with different modulation schemes in OFDM system to choose the target BER to perform the adaptive modulation. Higher data rate is achieved using adaptive modulation at target BER. The adaptive modulation is also studied for different Doppler frequencies. For higher Doppler frequency, the performance of adaptive modulation becomes challenging due to the ICI which affects the SNR estimation.



(a)



(b)

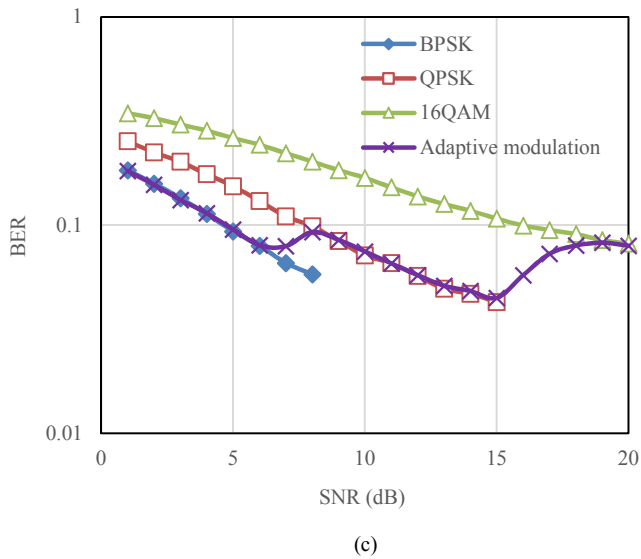


Fig. 5. BER performance of the proposed adaptive modulation scheme for Doppler frequency (a) 0.0139 Hz, (b) 0.1386 Hz and (c) 1.3856 Hz.

ACKNOWLEDGMENT

This research is supported by an Australian Government Research Training Program (RTP) Stipend and RTP Fee-Offset Scholarship through Curtin University.

REFERENCES

- [1] L. Wan, H. Zhou, X. Xu, Y. Huang, S. Zhou, Z. Shi and J.H. Cui, "Adaptive modulation and coding for underwater Acoustic OFDM", *IEEE J. of Oceanic Engineering*, vol. 40, issue 2, pp. 327-336, Apr. 2015.
- [2] P. Chen, Y. Rong, and S. Nordholm, "Pilot-subcarrier based impulsive noise mitigation for underwater acoustic OFDM systems," in *Proc. WUWNet*, 2016, Shanghai, China, Oct. 2016.
- [3] P. Chen, Y. Rong, S. Nordholm, A. Duncan and Z. He, "A LabView based implementation of real-time underwater acoustic OFDM system", in *Proc. 23rd Asia-Pacific Conference on Communications (APCC)*, pp. 730-734, Dec. 2017.
- [4] M. Stojanovic, "Underwater acoustic communications: design considerations on the physical layer," in *Proc. IEEE / IFIP Fifth Annual Conference on Wireless On demand Network Systems and Services (WONS)*, Jan. 2008.
- [5] M. Stojanovic and J. Preisig, "Underwater acoustic communication channels: Propagation models and statistical characterization", *IEEE Communications Magazine*, vol. 47, no. 1, pp. 84-89, Jan. 2009.
- [6] A. Radosevic, T. M. Duman, J. G. Proakis and M. Stojanovic, "Channel prediction for adaptive modulation in underwater acoustic communications," *OCEANS 2011 IEEE*, Spain, Santander, pp. 1-5, 2011.
- [7] M. Huang, S. Sun, E. Cheng, X. Kuai and X. Xu, "Joint interference mitigation with channel estimated in underwater acoustic OFDM system", *TELKOMNIKA*, vol. 11, no. 12, pp. 7423-7430, 2013.
- [8] S. Zhou and Z. Wang, "OFDM for underwater acoustic communications", John Wiley & Sons, Ltd, pp. 134, 2014.
- [9] J. Faezah and K. Sabira, "Adaptive modulation with OFDM system", *International Journal of Communication Networks and Information Security*, vol. 1, no. 2, Aug. 2009.